SCIENTIFIC REPORTS
nature research

OPEN

Enhancing quantum annealing performance by a degenerate two-level system

Shohei Watabe[1,2*], Yuya Seki[2] & Shiro Kawabata[2]

Quantum annealing is an innovative idea and method for avoiding the increase of the calculation cost of the combinatorial optimization problem. Since the combinatorial optimization problems are ubiquitous, quantum annealing machine with high efficiency and scalability will give an immeasurable impact on many fields. However, the conventional quantum annealing machine may not have a high success probability for finding the solution because the energy gap closes exponentially as a function of the system size. To propose an idea for finding high success probability is one of the most important issues. Here we show that a degenerate two-level system provides the higher success probability than the conventional spin-1/2 model in a weak longitudinal magnetic field region. The physics behind this is that the quantum annealing in this model can be reduced into that in the spin-1/2 model, where the effective longitudinal magnetic field may open the energy gap, which suppresses the Landau–Zener tunneling providing leakage of the ground state. We also present the success probability of the Λ-type system, which may show the higher success probability than the conventional spin-1/2 model.

Quantum annealing is an interesting approach for finding the optimal solution of combinatorial optimization problems by using the quantum effect[1–4]. The combinatorial optimization problems are ubiquitous in the real social world, therefore the spread of quantum annealing machine with high efficiency and high scalability will give impacts and benefits on many fields, such as an industry including drug design[5], financial portfolio problem[6], and traffic flow optimization[7]. After the commercialization of superconducting quantum annealing machine by D-Wave Systems inc.[8], several hardwares have been investigated and developed[9–13].

However, there are bottlenecks for implementing scalable quantum annealing machine; for the conventional and scalable quantum annealing machine may not have a high success probability for finding the solution of a combinatorial optimization problem because of the emergence of the first order phase transition, where the energy gap between ground state and the first exited state closes exponentially as a function of the system size[2]. In this case, it necessitates an exponentially long annealing time for finding the solution of the problem[14–16]. In the case of the second oder phase transition, on the other hand, an annealing time for finding the solution may scales polynomially as a function of the system size[17].

To propose an idea for finding high success probability is one of the most important and challenging issue in the field of quantum annealing. One of the approaches for obtaining the high success probability is to engineer the scheduling function for the driving Hamiltonian and the problem Hamiltonian, such as a monotonically increasing scheduling function satisfying the local adiabatic condition[18], the reverse quantum annealing[19] implemented in D-wave 2000Q[20], inhomogeneous sweeping out of local transverse magnetic fields[21,22], and a diabatic pulse application[23]. Another is to add an artificial additional Hamiltonian for suppressing the emergence of the excitations with avoiding the slowing down of annealing time, which is called shortcuts to adiabaticity by the counter-diabatic driving[24–27], and to add an additional Hamiltonian for avoiding the first order phase transition[17,28,29]. In this paper, we study the possibility of other approach: to employ a variant spin, such as a qudit, in the quantum annealing architecture.

Recently, two of the authors have studied the quantum phase transition in a degenerate two-level spin system, called the quantum Wajnflasz–Pick model, where an internal spin state is coupled to all the same energy internal states with a single coupling strength, and to all the different energy internal states with the other single coupling strength[30]. In the earlier study, this model is found to show a several kinds of phase transition while annealing;

[1]Department of Physics, Faculty of Science Division I, Tokyo University of Science, Shinjuku, Tokyo, 162-8601, Japan. [2]Nanoelectronics Research Institute, National Institute of Advanced Industrial Science and Technology (AIST), 1-1-1 Umezono, Tsukuba, Ibaraki, 305-8568, Japan. *email: shoheiwatabe@rs.tus.ac.jp

single or double first-order phase transitions as well as a single second-order phase transition, depending on an internal state coupling parameter[30], which suggests that the quantum annealing of this model may be controlled by an internal state tuning parameter. However, the study is based on the static statistical approach using the mean-field theory, because only the order of the phase transition has been interested in. Therefore, the enhancement of the success probability for quantum annealing based on degenerate two-level systems is not clear yet. Furthermore, they employed a fully-connected uniform interacting system, and it is unclear whether their idea works that a double (or even-number of) first-order phase transition while annealing would bring the system back into the ground state at the end of the annealing, where the even number of the Landau–Zener tunneling may happen with respect to the ground state.

In the present paper, we clarify the success probability of the quantum annealing in the quantum Wajnflasz–Pick model, focusing on (i) the Schrödinger dynamics, (ii) eigenenergies, and (iii) *non-uniform* effects of the spin-interaction as well as the longitudinal magnetic field. We find that the quantum Wajnflasz–Pick model is more efficient than the conventional spin-1/2 model in the weak longitudinal magnetic field region as well as in the strong coupling region between degenerate states. We also find that the quantum Wajnflasz–Pick model is reducible into a spin-1/2 model, where effect of the transverse magnetic field in the original Hamiltonian emerges in the reduced Hamiltonian not only as the effective transverse magnetic field but also as the effective longitudinal magnetic field. As a result, this model may provide the higher success probability in the case where the effective longitudinal magnetic field opens the energy gap between the ground state and the first excited state. We also evaluate the success probability in another variant spin, a Λ-type system[31–40], which has three internal levels. This model also shows the higher success probability than the conventional spin-1/2 model in the weak magnetic field region.

A multilevel system is ubiquitous, which can be seen, for example, in degenerate two-level systems in atoms[41,42], Λ-type atoms[31,32,34], Λ-, V-, Θ- and Δ-type systems in the superconducting circuits[33,35–40,43] as well as Λ-type systems in the nitrogen-vacancy centre in diamond[44]. We hope that insights of our results in the degenerate two-level system and knowledge of their reduced Hamiltonian inspire and promote further study as well as future engineering of quantum annealing.

Quantum Wajnflasz–Pick Model

A conventional quantum annealing consists of the spin-1/2 model, where the time dependent Hamiltonian is given by[1]

$$\hat{H}(s) = s\hat{H}_z + (1 - s)\hat{H}_x, \tag{1}$$

where $\hat{H}_{z,x}$ are a problem and driver Hamiltonian, respectively, and $s \equiv t/T$ is the time $t \in [0,\ T]$ scaled by the annealing time T. The problem Hamiltonian $\hat{H}_z$ with the number of spins N, which encodes the desired optimal solution, has a non-trivial ground state. In contrast, the driver Hamiltonian $\hat{H}_x$ has a trivial ground state, where the driver Hamiltonian $\hat{H}_x$ must not be commutable with the problem Hamiltonian $\hat{H}_z$. A problem Hamiltonian and driver Hamiltonian are typically given by

$$\hat{H}_z \equiv -\sum_{i\neq j}^{N} J_{ij}\hat{\sigma}_i^z\hat{\sigma}_j^z - \sum_{i}^{N} h_i^z\hat{\sigma}_i^z, \tag{2}$$

$$\hat{H}_x \equiv -\sum_{i}^{N} h_i^x\hat{\sigma}_i^x, \tag{3}$$

where $\hat{\sigma}^{x,z}$ are the Pauli matrices, J_{ij} is the coupling strength between spins, h_i^z is the local longitudinal magnetic field, and h_i^x is the local transverse magnetic field. The time-dependent total Hamiltonian $\hat{H}(s)$ gradually changes from the driver Hamiltonian $\hat{H}_x$ to the problem Hamiltonian $\hat{H}_z$. If the Hamiltonian changes sufficiently slowly, the quantum adiabatic theorem guarantees that the initial quantum ground state follows the instantaneous ground state of the total Hamiltonian[45]. We can thus finally obtain a non-trivial ground state of the problem Hamiltonian starting from the trivial ground state of the deriver Hamiltonian making use of the Schrödinger dynamics.

The quantum Wajnflasz–Pick model is a quantum version of the Wajnflasz–Pick model[46], which can describe one of the interacting degenerate two-level systems. In the language of the quantum annealing, the problem Hamiltonian and the driver Hamiltonian are respectively given by[30]

$$\hat{H}_z \equiv -\sum_{i\neq j}^{N} J_{ij}\hat{\tau}_i^z\hat{\tau}_j^z - \sum_{i}^{N} h_i^z\hat{\tau}_i^z, \tag{4}$$

$$\hat{H}_x \equiv -\sum_{i}^{N} h_i^x\hat{\tau}_i^x. \tag{5}$$

(Schematic picture of this model is shown in Fig. 1). The Hamiltonian of this model can be simply obtained by replacing the Pauli matrices $\hat{\sigma}^{x,z}$ in Eqs. (2) and (3) with the spin matrices of the quantum Wajnflasz-Pick model $\hat{\tau}^{x,z}$. The spin operator $\hat{\tau}^z$ is given by[30]

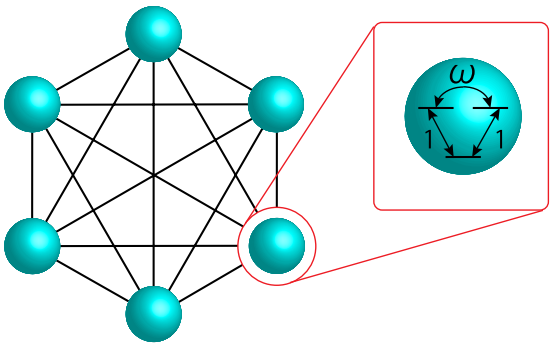

Figure 1. Schematic setup of an interacting degenerate two-level system, called the quantum Wajnflasz–Pick model.

$$\hat{\tau}^z \equiv \mathrm{diag}(\underbrace{+1, \ldots, +1}_{g_\mathrm{u}}, \underbrace{-1, \ldots, -1}_{g_\mathrm{l}}), \tag{6}$$

where $g_{\mathrm{u}(l)}$ is the number of the degeneracy of the upper (lower) states. The spin-operator $\hat{\tau}^x$ in the driver Hamiltonian is given by

$$\hat{\tau}^x \equiv \frac{1}{c}\begin{pmatrix} \mathbf{A}(g_\mathrm{u}) & \mathbf{1}(g_\mathrm{u}, g_\mathrm{l}) \\ \mathbf{1}(g_\mathrm{l}, g_\mathrm{u}) & \mathbf{A}(g_\mathrm{l}) \end{pmatrix}, \tag{7}$$

where $\mathbf{A}(l)$ is a $(l \times l)$ matrix with the off-diagonal term ω, given by

$$\mathbf{A}(l) \equiv \begin{pmatrix} 0 & \omega & \cdots & \omega \\ \omega^* & 0 & \ddots & \vdots \\ \vdots & \ddots & \ddots & \omega \\ \omega^* & \cdots & \omega^* & 0 \end{pmatrix}. \tag{8}$$

Here, ω is a parameter of the internal transition between the degenerated upper/lower states. The matrix $\mathbf{1}(m, n)$ is the $(m \times n)$ matrix, where all the elements is unity, which gives the transition between the upper and lower states. The constant c is the normalization factor, where the maximum eigenvalue is normalized to be $+1$, so as to be equal to the maximum eigenvalue of $\hat{\tau}^z$.

In the following, for the consistency to the earlier work[30], we consider a uniform transverse field $h_i^x \equiv 1$, and also take the parameter of the internal transition to be real $\omega = \omega^*$ with $\omega > -1$. In the case where $(g_\mathrm{u}, g_\mathrm{l}) = (2, 1)$, we have

$$\hat{\tau}^z \equiv \begin{pmatrix} 1 & 0 & 0 \\ 0 & 1 & 0 \\ 0 & 0 & -1 \end{pmatrix}, \quad \hat{\tau}^x \equiv \frac{1}{c}\begin{pmatrix} 0 & \omega & 1 \\ \omega & 0 & 1 \\ 1 & 1 & 0 \end{pmatrix}, \tag{9}$$

with $c = (\omega + \sqrt{8 + \omega^2})/2$, which is a kind of the Δ-type system[38].

In this paper, we employ the common sets of parameters in both quantum Wajnflasz–Pick model and the conventional spin-1/2 model, including the coupling strength J_{ij}, the magnetic fields $h_i^{z,x}$, and the annealing time T. By using these parameters, we can obtain the same spin configuration ($+1$ or -1) in the ground state of the problem Hamiltonian. We thus compare efficiency of these models from the success probability.

Schrödinger Dynamics

In order to numerically calculate the success probability of the quantum annealing, we employ the Crank–Nicholson method[47] for solving the Schrödinger equation

$$i\frac{d}{dt}|\Psi(t)\rangle = \hat{H}(t)|\Psi(t)\rangle. \tag{10}$$

In this method, the time-evolution of the wave function is calculated by using the Cayley's form[47]

$$|\Psi(t + \Delta t)\rangle = \frac{1 - i\hat{H}\Delta t/2}{1 + i\hat{H}\Delta t/2}|\Psi(t)\rangle. \tag{11}$$

Although the inverse matrix is needed, this method conserves the norm of the wave function and is second-order accurate in time[47].

We first consider the fully connected model, where the spin-spin coupling is ferromagnetic and the longitudinal magnetic field is uniform $h_i^z \equiv h$, which is consistent with the earlier work[30]. For example, in the case where

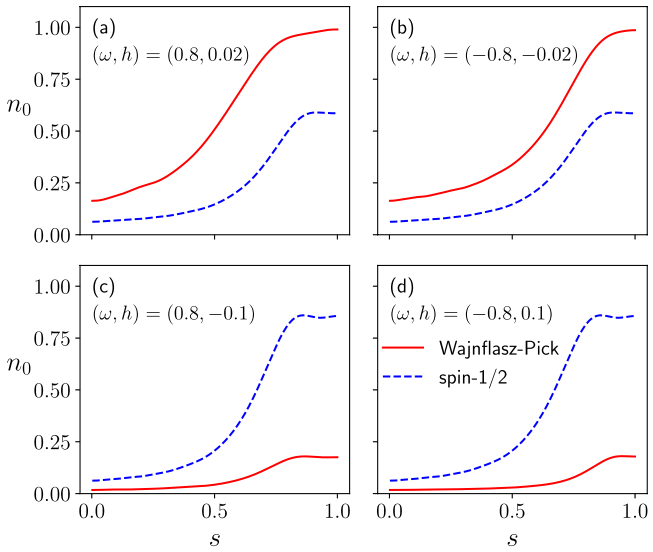

Figure 2. Population n_0 of the ground state of the problem Hamiltonian $\hat{H}_z$ in the quantum Wajnflasz–Pick model and that of the conventional spin-1/2 model, where $n_0 \equiv |\langle\Psi(t)|\Psi_0(T)\rangle|^2$. The scaled time s is given by $s \equiv t/T$. We employed the number of spins $N = 4$ both in the quantum Wajnflasz–Pick model and in the spin-1/2 model. We used the parameters $(g_u, g_l) = (2, 1)$, $J_{ij} = 1/N$, $h_i^x = 1$ and $T = 10$.

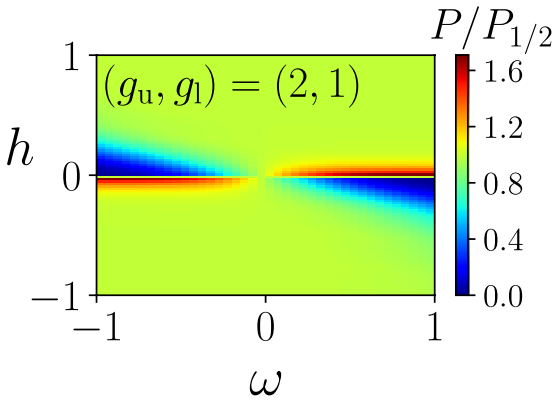

Figure 3. Success probability of a quantum Wajnflasz–Pick model P scaled by that of the conventional spin-1/2 model $P_{1/2}$ as a function of longitudinal magnetic field h and the coupling strength ω between degenerate internal states. The parameters are the same as those used in Fig. 2.

$(\omega, h) = (0.8, 0.02)$ and $(-0.8, -0.02)$ for $(g_u, g_l) = (2, 1)$, the time-dependence of the ground state population of the problem Hamiltonian, given by $n_0 \equiv |\langle\Psi(t)|\Psi_0(T)\rangle|^2$, clearly shows that this quantity in the quantum Wajnflasz–Pick model is greater than that in the conventional spin-1/2 model (Panels (a) and (b) in Fig. 2). Here, $|\Psi_0(T)\rangle$ is the ground state of the problem Hamiltonian, and $|\Psi(T)\rangle$ is the wave function obtained from the time-dependent Schrödinger equation. In the case where $(\omega, h) = (0.8, -0.1)$ and $(-0.8, 0.1)$ for $(g_u, g_l) = (2, 1)$, on the other hand, the ground state population of the problem Hamiltonian in the quantum Wajnflasz–Pick model is less than that in the spin-1/2 model (Panels (c) and (d) in Fig. 2).

Compare the success probability of the quantum Wajnflasz–Pick model, $P \equiv |\langle\Psi(T)|\Psi_0(T)\rangle|^2$, with that of the conventional spin-1/2 model denoted as $P_{1/2}$, where $|\Psi(T)\rangle$ is the final state obtained from the time-dependent Schrödinger equation. In almost all regions in the ω-h plane, efficiencies of both models are almost the same, where the ratio of the success probability of the quantum Wajnflasz–Pick model and that of the conventional spin-1/2 model is almost unity (Fig. 3). On the other hand, in the regime of the weak longitudinal magnetic field h, we can find higher or lower efficiency regions in the quantum Wajnflasz–Pick model, compared with the spin-1/2 model. In the spin glass model, a non-trivial state may emerge in the weak longitudinal magnetic field limit[48]. In a p-spin model where $p = 3, 5, 7, \ldots$, the energy gap is known to close exponentially and the first-order phase transition emerges in the absence of the longitudinal magnetic field[15]. In this sense, it is of interest that the quantum Wajnflasz–Pick model may provide the high efficiency in the weak longitudinal magnetic field region.

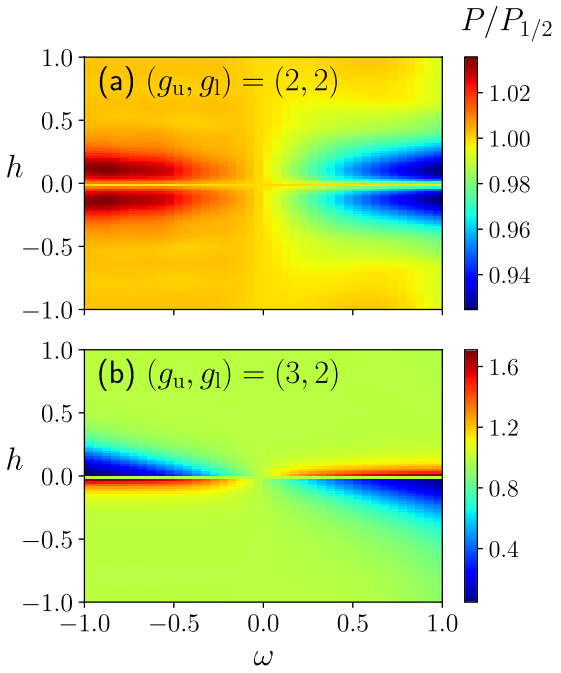

Figure 4. Success probability of a quantum Wajnflasz–Pick model P scaled by that of spin-1/2 model $P_{1/2}$. We consider the following degeneracy case: $(g_u, g_l) = (2, 2)$ in Panels (a) and $(g_u, g_l) = (3, 2)$ in Panels (b). We used $N = 4$, $J_{ij} = 1/N$, $h_i^x = 1$ and $T = 10$.

In the case where $(g_u, g_l) = (2, 2)$, where the numbers of upper and lower states are equal, the success probability of the quantum Wajnflasz–Pick model is almost equal to that of the conventional spin-1/2 model (Panel (a) in Fig. 4). In the case where $(g_u, g_l) = (3, 2)$, the success probability of the quantum Wajnflasz–Pick model is almost equal to that of the case where $(g_u, g_l) = (2, 1)$, where the differences between the number of the upper states and that of lower states are the same in both cases (Fig. 3 and Panel (b) in Fig. 4).

Eigenvalues

Eigenvalue spectrum of the instantaneous Hamiltonian may help to understand these higher or lower success probabilities of the quantum Wajnflasz–Pick model than that of spin-1/2 model, although eigenvalues of the instantaneous Hamiltonian shows tangled spaghetti structures (Fig. 5). For example, in the case where $(\omega, h) = (0.8, -0.1)$, the energy gap between the ground state and the first excited state clearly closes once, which causes the low success probability (Panel (c) in Fig. 5). In the case where $(\omega, h) = (0.8, 0.02)$, the ground state and the first excited state are finally merged at the annealing time, where the degeneracy would cause the high success probability (Panel (a) in Fig. 5). However, according to the following discussion, it will be found that the latter explanation would not be correct in the case where $(\omega, h) = (0.8, 0.02)$. From panels (b) and (d) in Fig. 5, many crossings of eigenvalues are found to emerge. It suggests that there are no matrix elements in some states, and we may find symmetry behind the present quantum Wajnflasz–Pick model, where the Hamiltonian would be block diagonalized by a unitary operator $\hat{U}$. Since the energy spectrum of the original quantum Wajnflasz-Pick model shows very complicated behavior, it would be better to find out the reason of the high/low success probability from the reduced Hamiltonian, which are truly relevant for the efficiency of the quantum annealing.

For example, in the case where $(g_u, g_l) = (2, 1)$, the single-spin Hamiltonian in the quantum Wajnflasz–Pick model is decomposable, where the irreducible representation is given by

$$\hat{U}^{-1}\hat{H}(s)\hat{U} = \begin{pmatrix} -h^+(s) & 0 & -2\sqrt{2}h'(s) \\ 0 & -h^-(s) & 0 \\ -2\sqrt{2}h'(s) & 0 & h^z s \end{pmatrix}, \tag{12}$$

for arbitrary values of s, by using the unitary operator

$$\hat{U} = \begin{pmatrix} \frac{1}{\sqrt{2}} & \frac{1}{\sqrt{2}} & 0 \\ \frac{1}{\sqrt{2}} & -\frac{1}{\sqrt{2}} & 0 \\ 0 & 0 & 1 \end{pmatrix}, \tag{13}$$

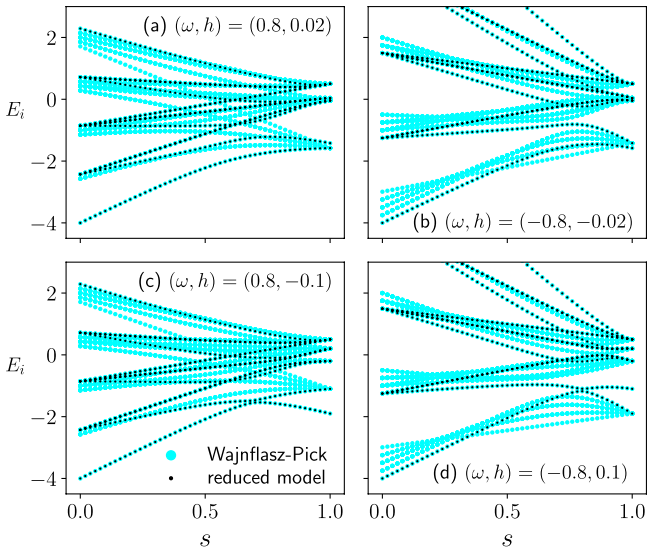

Figure 5. Eigenenergies of the instantaneous Hamiltonian in the quantum Wajnflasz–Pick model (blue) and those in the reduced spin-1/2 model (black) as a function of $s \equiv t/T$. The parameters are the same as those in Fig. 2.

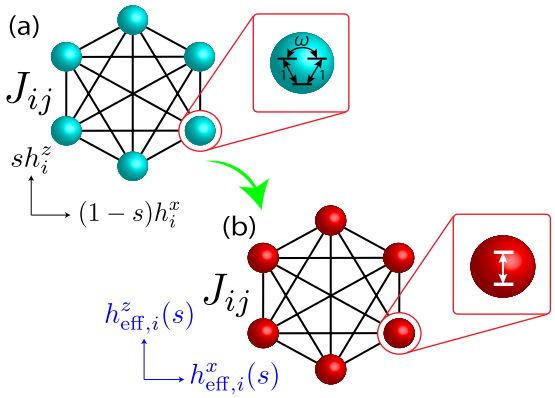

Figure 6. Schematics of an original quantum Wajnflasz–Pick model (**a**) and its reduced model (**b**).

where $h^{\pm}(s) \equiv h^z s \pm 2\omega h'(s)$, and $h'(s) \equiv (1-s)h^x/(2c)$. As a result, we may reduce a quantum annealing problem in the single-spin quantum Wajnflasz–Pick model into that of the spin-1/2 model, the Hamiltonian of which is given in the form

$$\hat{\mathscr{H}}(s) = -[h^z s + \omega h'(s)]\hat{\sigma}^z - 2\sqrt{2}h'(s)\hat{\sigma}^x - \omega h'(s). \tag{14}$$

Since the initial ground state of the single-spin Hamiltonian is given by $|\Psi(s=0)\rangle \propto (c/2,\ c/2,\ 1)^{\mathrm{T}}$ in the original quantum Wajnflasz–Pick model, this state can be mapped to $\hat{U}|\Psi(s=0)\rangle \propto (c/\sqrt{2},\ 0,\ 1)^{\mathrm{T}}$. It indicates that the initial ground state $\hat{U}|\Psi(s=0)\rangle$ can be also projected to the Hilbert space of the reduced Hamiltonian $\hat{\mathscr{H}}(s)$.

This reduction of the single-spin problem in the case where $(g_{\mathrm{u}},\ g_{\mathrm{l}}) = (2,\ 1)$ can be generalized to an interacting N-spin problem (Fig. 6). A quantum annealing problem of the original quantum Wajnflasz–Pick model is reduced into that of the spin-1/2 model, given in the form

$$\begin{aligned}\hat{\mathscr{H}}(s) \ = \ & s\left(-\sum_{i<j} J_{ij}\sigma_i^z\sigma_j^z\right) - \sum_i h^z_{\mathrm{eff},i}(s)\sigma_i^z \\ & - \sum_i h^x_{\mathrm{eff},i}(s)\sigma_i^x - \sum_i \omega h'_i(s),\end{aligned} \tag{15}$$

where

$$h^z_{\mathrm{eff},i}(s) \equiv h_i^z s + \omega h'_i(s), \tag{16}$$

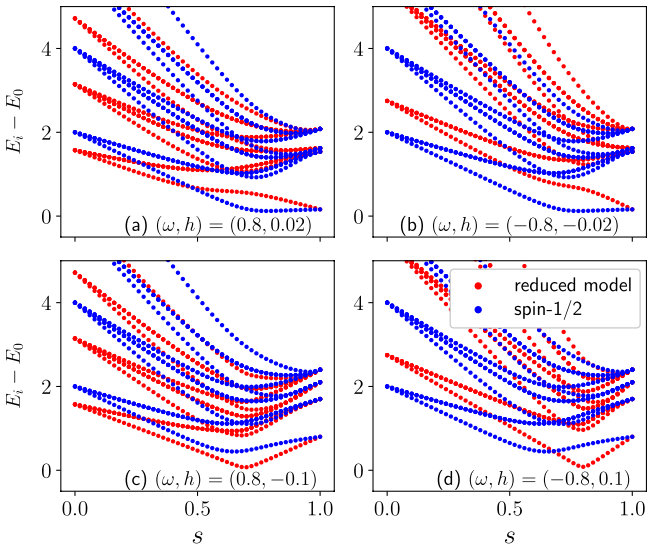

Figure 7. Excited state energies measured from the ground state energy of the instantaneous Hamiltonian in the reduced model (red) and those in the conventional spin-1/2 model (blue). The parameters are the same as those in Fig. 2.

$$h^x_{\mathrm{eff},i}(s) \equiv 2\sqrt{2}h'_i(s), \tag{17}$$

with

$$h'_i(s) \equiv \frac{(1-s)h_i^x}{2c}. \tag{18}$$

As in the single-spin case, the initial ground state of the original N-spin quantum Wajnflasz–Pick model can be also projected to the Hilbert space of the reduced Hamiltonian (15). The coupling J_{ij} in the reduced Hamiltonian is the same as that of the original Wajnflasz–Pick model. The effective longitudinal magnetic field $h^z_{\mathrm{eff},i}$ in the reduced Hamiltonian also reaches the same value as that of the original Wajnflasz–Pick model at the end of the annealing: $h^z_{\mathrm{eff},i}(s=1) = h_i^z$. Eigenvalues of the reduced spin-1/2 model exactly trace eigenvalues in the original Wajnflasz–Pick model (Fig. 5). The time-dependence of the ground state population of the problem Hamiltonian is confirmed to show the completely same behavior between the reduced model and the original model.

This effective model clearly explains behavior of success probability of the quantum Wajnflasz–Pick model shown in Fig. 3. Note that the coefficient c is a positive real number such that the maximum eigenvalue of τ^x is unity, and we take $h_i^x = 1$. Then, $h'_i(s) \geq 0$ always holds during the annealing time $0 \leq s \leq 1$. In the case where the longitudinal magnetic field h_i^z is very large, $|h_i^z| \gg |\omega| h'_i(0)$, the effect of the original longitudinal magnetic field h_i^z is dominant compared with the effective additional term $\omega h'_i(s)$ except at the very early stage of the annealing $s \ll |\omega h'_i(0)/h_i^z|$. In this case, the problem Hamiltonian in the reduced model is almost the same as that in the conventional spin-1/2 model in Eq. (2). As a result, the success probability of the quantum Wajnflasz–Pick model is almost the same as that of the conventional spin-1/2 model, which provides $P \simeq P_{1/2}$.

In the case where the original longitudinal magnetic field h_i^z is not large, the effective additional longitudinal magnetic field $\omega h'_i(s)$ cannot be neglected compared with h_i^z. When the effective additional field is in the same direction as the original longitudinal field, the total effective longitudinal magnetic field $h^z_{\mathrm{eff},i}(s)$ is enhanced, which opens the energy gap between the ground state and the first excited state (Panels (a) and (b) in Fig. 7). This region is given by the condition $\omega h_i^z > 0$, which is consistent with the result shown in Fig. 3. As a result, the success probability of the quantum Wajnflasz–Pick model become superior to that of the conventional spin-1/2 model. When the effective additional field is in the opposite direction to the original longitudinal field, the total effective longitudinal magnetic field $h^z_{\mathrm{eff},i}(s)$ is diminished, which closes the energy gap between the ground state and the first excited state (Panels (c) and (d) in Fig. 7). This region is given by the condition $\omega h_i^z < 0$, which is consistent with the result shown in Fig. 3. As a result, the success probability of the quantum Wajnflasz–Pick model become inferior to that of the conventional spin-1/2 model.

Behavior of success probability is also explained by the reference of the annealing time[49]

$$\mathscr{T} \equiv \max_s \left[\frac{b(s)}{\Delta(s)^2} \right], \tag{19}$$

where

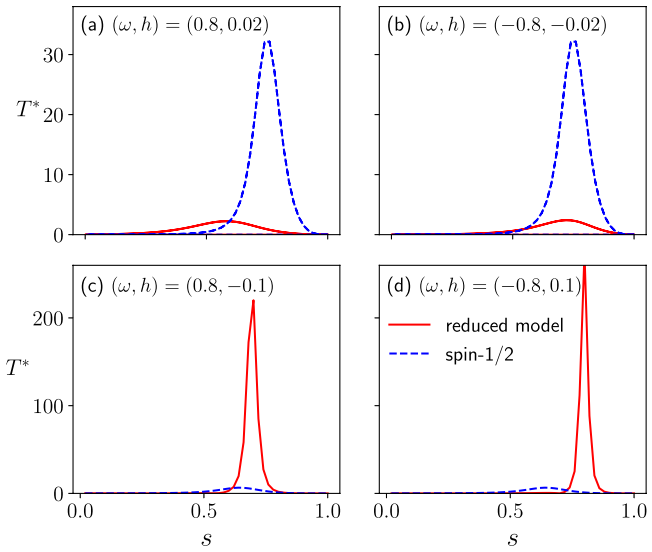

Figure 8. Instantaneous reference annealing time $T^* \equiv b(s)/\Delta^2(s)$ as a function of the scaled time s. The parameters are the same as those in Fig. 2.

$$b(s) \equiv \left| \left\langle \Psi_1(s) \left| \frac{d\hat{H}(s)}{ds} \right| \Psi_0(s) \right\rangle \right|, \tag{20}$$

$$\Delta(s) \equiv E_1(s) - E_0(s). \tag{21}$$

Here, $|\Psi_{0(1)}(s)\rangle$ and $E_{0(1)}(s)$ are the wave functions and eigenenergies of the ground (first-excited) state with respect to the instantaneous Hamiltonian, respectively. Annealing machine needs the annealing time T much larger than $\mathscr{T}$. Let $T^* \equiv b(s)/\Delta^2(s)$ be an instantaneous reference time of the annealing. The maximum value of this time T^* in the reduced Wajnflasz–Pick model given in (15) is suppressed compared with that of the conventional spin-1/2 model, where the effective additional field $\omega h'_i(s)$ is in the same direction as the original longitudinal field h_i^z (Panels (a) and (b) in Fig. 8). It is consistent with the case where the quantum Wajnflasz–Pick model is more efficient than the conventional spin-1/2 model in the region where $\omega h_i^z > 0$ (Fig. 3). The maximum value of T^* in the effective Wajnflasz–Pick model has larger values than that of the spin-1/2 model, where the effective additional field $\omega h'_i(s)$ is in the opposite direction to the original longitudinal field h_i^z (Panels (c) and (d) in Fig. 8). It is consistent with the case where the quantum Wajnflasz–Pick model is less efficient than the conventional spin-1/2 model in the region where $\omega h_i^z < 0$ (Fig. 3).

In order to perform the scaling analysis of the minimum energy gap $\Delta_{\min} \equiv \min [E_1(s) - E_0(s)]$, we consider the p-spin model in the absence of the longitudinal magnetic field:

$$\hat{H}(s) = s\Big(-\frac{1}{N^{p-1}} \sum_{i_1,\ldots,i_p}^{N} \hat{\tau}_{i_1}^z \cdots \hat{\tau}_{i_p}^z \Big) + (1-s)\Big(-h^x \sum_{i}^{N} \hat{\tau}_i^x \Big), \tag{22}$$

where the transverse magnetic field is homogeneous. Replacement of $\tau_i^{x,y}$ with $\sigma_i^{x,y}$ provides the conventional p -spin model, where the first order phase transition emerges, and the minimum energy gap is known to close exponentially as N increases in the case where p is odd[15]. After mapping to the subspace spanned by the spin-1/2 model, the reduced Hamiltonian of the quantum Wajnflasz–Pick model with $(g_u, g_l) = (2, 1)$ can be given by

$$\hat{\mathscr{H}}(s) = -s\frac{1}{N^{p-1}} \sum_{i_1,\ldots,i_p}^{N} \hat{\sigma}_{i_1}^z \cdots \hat{\sigma}_{i_p}^z - (1-s)\Gamma^z \sum_{i}^{N} \hat{\sigma}_i^z - (1-s)\Gamma^x \sum_{i}^{N} \hat{\sigma}_i^x, \tag{23}$$

$$= -s\frac{1}{N^{p-1}} (\hat{M}^z)^p - (1-s)\Gamma^z \hat{M}^z - (1-s)\Gamma^x \hat{M}^x, \tag{24}$$

up to the constant energy shift, where $\Gamma^z \equiv \omega h^x/(2c)$, $\Gamma^x \equiv \sqrt{2}\, h^x/c$, and $\hat{M}^{z,x} \equiv \sum_i^N \hat{\sigma}_i^{z,x}$. By using the commutation relation $[\hat{\sigma}_i^x, \hat{\sigma}_j^z] = 2i\hat{\sigma}_i^z \delta_{ij}$ and by following the standard argument of the angular momentum, where the total spin $\hat{\mathbf{M}}^2 \equiv (\hat{M}^x)^2 + (\hat{M}^y)^2 + (\hat{M}^z)^2$ conserves, the Hilbert space can be spanned by states $|J, M\rangle$, where $\hat{\mathbf{M}}^2 |J, M\rangle = J(J+2)|J, M\rangle$ and $\hat{M}^z |J, M\rangle = M|J, M\rangle$ with $M = -J, -J+2, \cdots, J-2, J$. The diagonal elements

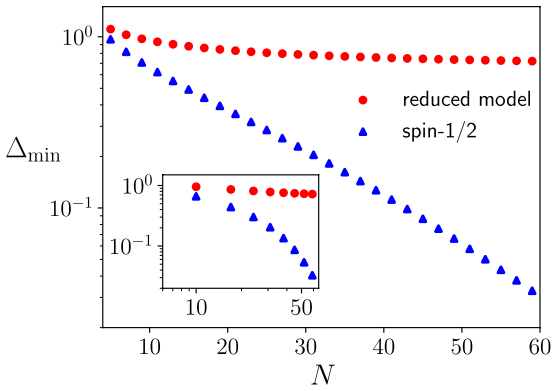

Figure 9. Minimum energy gap as a function of the number of spins N on a linear-log scale (a log-log scale in the inset). The minimum energy gap is obtained from the exact diagonalization of the ferromagnetic p-spin model with $p = 3$. We have used $\omega = 0.8$ and $h^x = 1$.

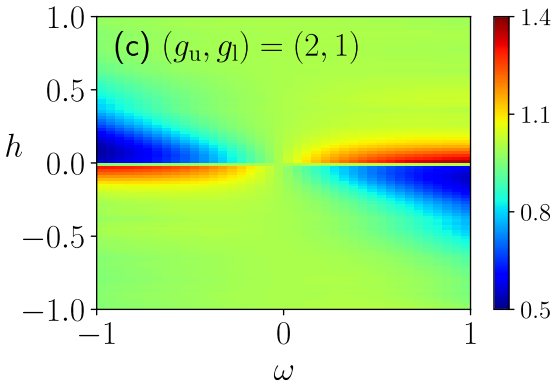

Figure 10. Averaged success probability of a quantum Wajnflasz–Pick model P scaled by that of spin-1/2 model $P_{1/2}$ in a randomly generated coupling strength case. We employed the coupling strength J_{ij} randomly generated from the gaussian distribution function, where the mean is zero and the variance is $1/N$. We used $N = 4, h_i^x = 1$ and $T = 10$. The success probabilities P and $P_{1/2}$ are averaged values of 100 samplings in each data point.

of this Hamiltonian is given by $\mathscr{H}_{MM} = -sM^p/(N^{p-1}) - (1-s)\Gamma^z M$, and the off-diagonal elements are $\mathscr{H}_{M,M\pm2} = -(1-s)\Gamma^x\sqrt{J(J+2) - M(M\pm2)}/2$. Since the ground state of this model is given by the case $J = N$, we diagonalize the $(N+1) \times (N+1)$ matrix of the reduced Hamiltonian. We compare the minimum energy gap of this model reduced from the quantum Wajnflasz–Pick model with that of the conventional p-spin model composed of the spin-1/2 system (Eq. (24) with $\Gamma^z = 0$ and $\Gamma^x = h^x$). Figure 9 clearly shows that the minimum energy gap closes exponentially in the conventional spin-1/2 model, and the gap closes polynomially in the model reduced from the quantum Wajnflasz–Pick model. This polynomial gap closing originates from the emergence of the effective longitudinal magnetic field in the reduced model: $\Gamma^z = \omega h^x/(2c) \neq 0$.

Random Coupling

In the random spin-spin coupling case, where J_{ij} are randomly generated by the gaussian distribution function[50]

$$P(J_{ij}) = \sqrt{\frac{N}{2\pi}}\exp\left(-\frac{N}{2}J_{ij}^2\right), \tag{25}$$

the density plot of the mean-value of the success probability is similar to the uniform coupling case. The maximum (minimum) value of the success probability is, however, suppressed (increased) compared with the uniform coupling case (Fig. 10). The variances of the success probability of the quantum Wajnflasz–Pick model are almost ranged from 0.03 to 0.06 in the first and third orthants in the ω-h plane, where the higher success probability may be obtained than the conventional spin-1/2 model. They are almost ranged from 0.02 to 0.15 in the second and forth orthants in the ω-h plane, where the lower success probability may be obtained. In the spin-1/2 model, the variance of the success probability is almost within the range from 0.03 to 0.06 in all the orthants.

The discussion above is in the case for a uniform longitudinal magnetic field. In the following, we discuss the case of random longitudinal magnetic fields h_i^z in addition to the random interactions J_{ij}. The success probabilities P and $P_{1/2}$ are almost equal in the weak internal state coupling case ($\omega = \pm 0.1$ in Fig. 11). In the strong internal

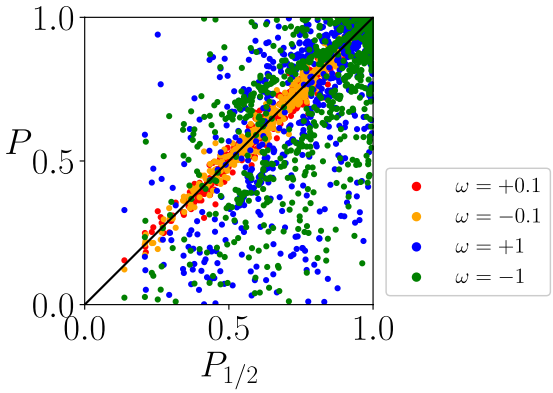

Figure 11. Success probability P of the quantum Wajnflasz–Pick model vs. success probability $P_{1/2}$ of the conventional spin-1/2 model. We take 1000 samples of problem hamiltonian with the random coupling strength J_{ij} as well as the random longitudinal magnetic field h_i^z, both of which are generated from the standard Gaussian distribution. The means of J_{ij} and h_i^z are zeros, and the variances are $1/N$ and $1/\sqrt{2}$, respectively. For each problem set, we consider four cases $\omega = \pm 0.1$ and ± 1. We used $(g_u, g_l) = (2, 1), N = 4, h_i^x = 1$ and $T = 10$.

state coupling case ($\omega = \pm 1$ in Fig. 11), the distribution is broaden. Although we can find cases where the conventional spin-1/2 model is superior to the quantum Wajnflasz–Pick model, we can also find many cases where the quantum Wajnflasz–Pick model is superior to the conventional spin-1/2 model, where the success probability is close to the unity compared with the conventional spin-1/2 model.

In these random coupling cases, it may not be definitely concluded that the quantum Wajnflasz–Pick model is always more efficient than the conventional spin-1/2 model. The variance is relatively large, and there are cases where the quantum Wajnflasz–Pick model is inferior to the conventional spin-1/2 model (Fig. 11). However, we can find many cases where the quantum Wajnflasz–Pick model is possibly more efficient than the conventional spin-1/2 model. In the quantum Wajnflasz–Pick model and its reduced model, we have chances to find a better solution of the combinatorial optimization problem. In real annealing machines, we can extract a better solution after performing many sampling experiments by tuning ω.

Discussion

In the case where $(g_u, g_l) = (2, 1)$, the spin matrix in the quantum Wajnflasz–Pick model is represented by a (3×3)-matrix, which suggests that the quantum Wajnflasz–Pick model in this case may be mapped into the model represented by the spin-1 matrices given by

$$\hat{S}^x = \frac{1}{\sqrt{2}}\begin{pmatrix} 0 & 1 & 0 \\ 1 & 0 & 1 \\ 0 & 1 & 0 \end{pmatrix}, \quad \hat{S}^y = \frac{i}{\sqrt{2}}\begin{pmatrix} 0 & -1 & 0 \\ 1 & 0 & -1 \\ 0 & 1 & 0 \end{pmatrix}, \quad \hat{S}^z = \begin{pmatrix} 1 & 0 & 0 \\ 0 & 0 & 0 \\ 0 & 0 & -1 \end{pmatrix}. \tag{26}$$

Indeed, after we interchange elements of second and third rows in the spin matrices defined in Eq. (9) in the case where $(g_u, g_l) = (2, 1)$, as well as we interchange elements of second and third columns, simultaneously, we find the following maps

$$\hat{\tau}^z \mapsto \hat{q}^z \equiv \frac{2}{\sqrt{3}}\hat{Q}^{3z^2-r^2} + \frac{1}{3}, \tag{27}$$

$$\hat{\tau}^x \mapsto \hat{q}^x \equiv \frac{1}{c}\left[\sqrt{2}\hat{S}^x + \Re\omega\hat{Q}^{x^2-y^2} - \Im\omega\hat{Q}^{xy}\right], \tag{28}$$

where we have introduced quadrupolar operators[51,52]

$$\hat{Q}^{3z^2-r^2} \equiv \frac{1}{\sqrt{3}}[2(\hat{S}^z)^2 - (\hat{S}^x)^2 - (\hat{S}^y)^2], \tag{29}$$

$$\hat{Q}^{x^2-y^2} \equiv (\hat{S}^x)^2 - (\hat{S}^y)^2, \tag{30}$$

$$\hat{Q}^{xy} \equiv \hat{S}^x\hat{S}^y + \hat{S}^y\hat{S}^x, \tag{31}$$

and $\Re\omega$ ($\Im\omega$) is the real (imaginary) part of ω. Since $[\hat{q}^z, (\hat{S}^x)^2] = 0$ and $[\hat{q}^x, (\hat{S}^x)^2] = i(\Im\omega/c)\hat{S}^x$ hold, we find that $(\hat{S}^x)^2$ is the operator of the conserved quantity in the case where the parameter ω is a real number. The coupling of $\hat{\tau}_i^z\hat{\tau}_{j(\neq i)}^z$ is mapped into the interaction $\hat{q}_i^z\hat{q}_{j(\neq i)}^z$, which is a kind of the biquadratic interaction with respect to the

spin. In short, the interacting quantum Wajnflasz–Pick model with $(g_u, g_l) = (2, 1)$ can be mapped into the spin-1 model with an artificial biquadratic interaction. In particular, in the case where $\omega \in \mathbb{R}$, there is the hidden symmetry related to $(\hat{S}^x)^2$, which indicates that the quantum Wajnflasz–Pick model is reducible in this case.

It is general that an interacting quantum Wajnflasz–Pick model is reducible to the conventional spin-1/2 model. It holds for an arbitrary number of the degeneracy (g_u, g_l) and at an arbitrary time s, which can be proven in the case where the parameter ω is a real number and the condition $\omega > -1$ holds. In Supplementary Information, we show that the Hamiltonian of the interacting quantum Wajnflasz–Pick model with arbitrary (g_u, g_l) can be projected to the spin-1/2 model, and the initial ground state in the original quantum Wajnflasz–Pick Hamiltonian is also projected to the reduced Hilbert space. It indicates that the quantum annealing in the quantum Wajnflasz–Pick model can be always described by the reduced Hamiltonian.

As shown in Supplementary Information, this projection holds not only in the 2-body interacting quantum Wajnflasz–Pick model, but also in the N-body interacting model. It indicates that if the quantum Wajnflasz–Pick model is embedded into the Lechner–Hauke–Zoller (LHZ) architecture[53,54], it can be also projected into the LHZ architecture composed of the spin-1/2 model, where the effective additional magnetic fields may emerge. The present quantum Wajnflasz–Pick model is a degenerate two-level system in the presence of the transverse magnetic field. The possibility of the implementation of the degenerate two-level system has been discussed for the D_2 line of ^{87}Rb[41,42]. The quantum Wajnflasz–Pick model is also similar to the Δ-type cyclic artificial atom in the superconducting circuit[38,43]. In the Δ-type artificial atom, the population is controllable by making use of the amplitudes and/or phases of microwave pulses, where the amplitudes alone controls the population in the conventional three-level system (Λ-type system)[43]. However, the Δ-type system in the superconducting circuit is not an exactly degenerate two-level system. With this regard, it may be difficult to directly implement our model in the Δ-type cyclic artificial atom in the superconducting circuit. Actually, it may be feasible to employ the spin-1/2 model with the scheduling function inspired by the quantum Wajnflasz–Pick model, in the case where the Schrödinger dynamics without the dissipation holds.

The quantum Wajnflasz–Pick model is one of the qudit models, which is a kind of the artificial Δ-type system[38,43] in the case where $(g_u, g_l) = (2, 1)$. The question naturally arises whether the Λ-type system also shows the higher success probability than the conventional spin-1/2 model. The spin matrix of the Λ-type system we employ here is given by

$$\hat{\tau}^z = \begin{pmatrix} 0 & 0 & 0 \\ 0 & 1 & 0 \\ 0 & 0 & \varepsilon \end{pmatrix}, \quad \hat{\tau}^x = \frac{1}{c}\begin{pmatrix} 0 & \kappa & 0 \\ \kappa & 0 & 1 \\ 0 & 1 & 0 \end{pmatrix}, \tag{32}$$

where we take $|\varepsilon| \leq 1$, and the coefficient $c \equiv \sqrt{1 + \kappa^2}$ is a normalization factor so as the maximum eigenvalues of $\hat{\tau}^{x,z}$ are unity. The Hamiltonian of the quantum annealing with the Λ-type system is given by Eqs. (1), (4) and (5), where $\hat{\tau}^{x,z}$ are replaced with those given in (32). The success probability in the Λ-type system is found to be higher than that in the conventional spin-1/2 model, in the case where ε is small in the weak longitudinal magnetic field region, which is similar to the case of the quantum Wajnflasz–Pick model (Panels (a) and (b) in Fig. 12). When ε is large, on the other hand, the success probability is drastically suppressed (Panel (c) in Fig. 12). In the case of a single Λ-spin system with $\varepsilon = 0$, which corresponds to a degenerate two-level system, the unitary transformation

$$\hat{U} = \frac{1}{c}\begin{pmatrix} \kappa & 0 & 1 \\ 0 & 1 & 0 \\ 1 & 0 & -\kappa \end{pmatrix} \tag{33}$$

can map the Hamiltonian $\hat{H}(s) = -sh^z\hat{\tau}^z - (1-s)h^x\hat{\tau}^x$ to the following block diagonal form:

$$\hat{U}^{-1}\hat{H}(s)\hat{U} = \begin{pmatrix} 0 & -(1-s)h^x & 0 \\ -(1-s)h^x & -sh^z & 0 \\ 0 & 0 & 0 \end{pmatrix}. \tag{34}$$

As a result, after exchanging the first and second columns and also the first and second rows, we may reduce a quantum annealing problem in this Λ-spin model into that of the spin-1/2 model, the Hamiltonian of which is given by $\hat{\mathscr{H}}(s) = -sh^z\sigma^z/2 - (1-s)h^x\sigma^x - sh^z/2$. Although the Λ-type system may provide the higher success probability than the conventional spin-1/2 model, the effect of dark states (never employed states) on the quantum annealing in the general Λ-spin case and its reduction to the spin-1/2 model in the many-spin system would be important issues for future study.

To summarize, we have demonstrated that qudit models, such as the quantum Wajnflasz–Pick model as well as the Λ-type system, may provide the higher success probability than the conventional spin-1/2 model in the weak magnetic field region. We have analytically shown that the quantum Wajnflasz–Pick model can be reduced into the spin-1/2 model, where effect of the transverse magnetic field in the original Hamiltonian emerges as the effective additional longitudinal magnetic field in the reduced Hamiltonian, which possibly opens the energy gap between the ground state and the first excited state in the reduced Hamiltonian. Since qubits have experimental advantages for the manipulation, the direct implementation of the reduced spin-1/2 model may be convenient for the quantum annealing. On the other hand, the reduction to the subspace in terms of the spin-1/2 model is useful only in the case where we focus on the Schrödinger dynamics. If we consider the dissipation as a realistic system, the transition between the subspaces emerges. The efficiency of the quantum annealing in this system is open for further study.

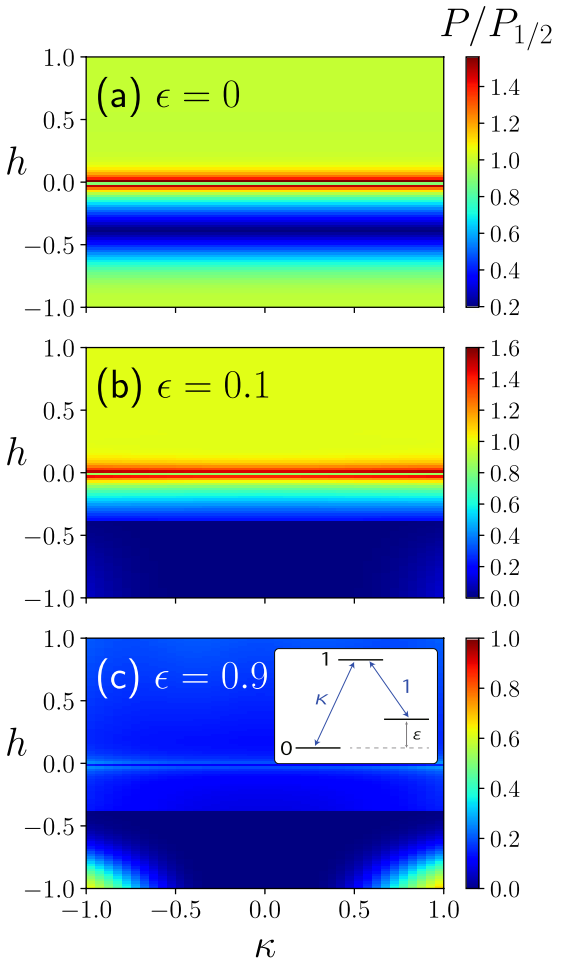

Figure 12. Success probability P of the Λ-type system in the h-κ plane, compared with that of the conventional spin-1/2 model $P_{1/2}$. The number of spin both in the Λ-type system and in the spin-1/2 model is $N = 4$. We used the parameter sets $J_{ij} = 1/N, h_i^x = 1$ and $T = 10$.

Conclusions

We studied the performance of the quantum annealing constructed by one of the degenerate two-level systems, called the quantum Wajnflasz–Pick model. This model shows the higher success probability than the conventional spin-1/2 model in the region where the longitudinal magnetic field is weak. The physics behind this is that the quantum annealing of this model can be reduced into that of the spin-1/2 model, where the effective longitudinal magnetic field in the reduced Hamiltonian may open the energy gap between the ground state and the first excited state, which gives rise to the suppression of the Landau–Zener transition. The reduction of the quantum Wajnflasz–Pick model to the spin-1/2 model is general at an arbitrary time as well as in an arbitrary number of degeneracies. We also demonstrated that the Λ-type system also shows the higher success probability than the conventional spin-1/2 model in the weak magnetic field regions. We hope that studying quantum annealing with variant spins, and utilizing the insight of their reduced model will promote further development of high performance quantum annealer.

Received: 9 July 2019; Accepted: 16 December 2019;
Published online: 10 January 2020

References

1. Kadowaki, T. & Nishimori, H. Quantum annealing in the transverse Ising model. *Phys Rev E* **58**, 5355–5363 (1998).
2. Albash, T. & Lidar, D. A. Adiabatic quantum computation. *Reviews of Modern Physics* **90**, 015002 (2019).
3. Farhi, E., Goldstone, J., Gutmann, S. & Sipser, M. Quantum computation by adiabatic evolution, quant-ph/0001106 (2000).
4. Farhi, E. *et al.* A Quantum Adiabatic Evolution Algorithm Applied to Random Instances of an NP-Complete Problem. *Science* **292**, 472–475 (2001).
5. Sakaguchi, H. *et al.* Boltzmann Sampling by Degenerate Optical Parametric Oscillator Network for Structure-Based Virtual Screening. *Entropy* **18**, 365 (2016).
6. Rosenberg, G. *et al.* Solving the Optimal Trading Trajectory Problem Using a Quantum Annealer. *IEEE Journal of Selected Topics in Signal Processing* **10**, 1053–1060 (2016).
7. Neukart, F. *et al.* Traffic Flow Optimization Using a Quantum Annealer. *Frontiers in ICT* **4**, 126 (2017).
8. https://www.dwavesys.com.
9. Barends, R. *et al.* Digitized adiabatic quantum computing with a superconducting circuit. *Nature* **534**, 222 (2016).

10. Rosenberg, D. *et al*. 3D integrated superconducting qubits. *npj Quantum Information* **3**, 1 (2017).
11. Novikov, S. *et al*. Exploring More-Coherent Quantum Annealing. In *2018 IEEE International Conference on Rebooting Computing (ICRC)*, 1–7 (IEEE, 2018).
12. Maezawa, M. *et al*. Toward Practical-Scale Quantum Annealing Machine for Prime Factoring. *Journal of the Physical Society of Japan* **88**, 061012 (2019).
13. Mukai, H., Tomonaga, A. & Tsai, J.-S. Superconducting Quantum Annealing Architecture with LC Resonators. *Journal of the Physical Society of Japan* **88**, 061011 (2019).
14. Žnidarič, M. & Horvat, M. Exponential complexity of an adiabatic algorithm for an NP-complete problem. *Physical Review A* **73**, 022329 (2006).
15. Jörg, T., Krzakala, F., Kurchan, J., Maggs, A. C. & Pujos, J. Energy gaps in quantum first-order mean-field–like transitions: The problems that quantum annealing cannot solve. *EPL (Europhysics Letters)* **89**, 40004 (2010).
16. Jörg, T., Krzakala, F., Semerjian, G. & Zamponi, F. First-Order Transitions and the Performance of Quantum Algorithms in Random Optimization Problems. *Physical Review Letters* **104**, 207206 (2010).
17. Seki, Y. & Nishimori, H. Quantum annealing with antiferromagnetic fluctuations. *Phys. Rev. E* **85**, 051112 (2012).
18. Roland, J. & Cerf, N. J. Quantum search by local adiabatic evolution. *Physical Review A* **65**, 042308 (2002).
19. Perdomo-Ortiz, A., Venegas-Andraca, S. E. & Aspuru-Guzik, A. A study of heuristic guesses for adiabatic quantum computation. *Quantum Information Processing* **10**, 33–52 (2010).
20. https://www.dwavesys.com/sites/default/files/14-1018A-A_Reverse_Quantum_Annealing_for_Local_Refinement_of_Solutions.pdf (2017).
21. Susa, Y., Yamashiro, Y., Yamamoto, M. & Nishimori, H. Exponential Speedup of Quantum Annealing by Inhomogeneous Driving of the Transverse Field. *Journal of the Physical Society of Japan* **87**, 023002 (2018).
22. Susa, Y. *et al*. Quantum annealing of the *p*-spin model under inhomogeneous transverse field driving. *Physical Review A* **98**, 042326 (2018).
23. Karanikolas, V. & Kawabata, S. Improved performance of quantum annealing by a diabatic pulse application, arXiv:1806.08517 (2018).
24. Campo, A. D. & Boshier, M. G. Shortcuts to adiabaticity in a time-dependent box. *Scientific Reports* **2**, 648 (2012).
25. del Campo, A. Shortcuts to Adiabaticity by Counterdiabatic Driving. *Physical Review Letters* **111**, 100502 (2013).
26. Sels, D. & Polkovnikov, A. Minimizing irreversible losses in quantum systems by local counterdiabatic driving. *Proceedings of the National Academy of Sciences* **114**, E3909–E3916 (2017).
27. Hartmann, A. & Lechner, W. Rapid counter-diabatic sweeps in lattice gauge adiabatic quantum computing. *New Journal of Physics* **21**, 043025 (2019).
28. Seoane, B. & Nishimori, H. Many-body transverse interactions in the quantum annealing of thep-spin ferromagnet. *Journal of Physics A: Mathematical and Theoretical* **45**, 435301 (2012).
29. Seki, Y. & Nishimori, H. Quantum annealing with antiferromagnetic transverse interactions for the Hopfield model. *Journal of Physics A: Mathematical and Theoretical* **48**, 335301 (2015).
30. Seki, Y., Tanaka, S. & Kawabata, S. Quantum Phase Transition in Fully Connected Quantum Wajnflasz–Pick Model. *Journal of the Physical Society of Japan* **88**, 054006 (2019).
31. Cirac, J. I., Zoller, P., Kimble, H. J. & Mabuchi, H. Quantum State Transfer and Entanglement Distribution among Distant Nodes in a Quantum Network. *Physical Review Letters* **78**, 3221–3224 (1997).
32. Duan, L. M., Lukin, M. D., Cirac, J. I. & Zoller, P. Long-distance quantum communication with atomic ensembles and linear optics. *Nature* **414**, 413–418 (2001).
33. Zhou, Z., Chu, S.-I. & Han, S. Quantum computing with superconducting devices: A three-level SQUID qubit. *Physical Review B* **66**, 054527 (2002).
34. Sun, C. P., Li, Y. & Liu, X. F. Quasi-Spin-Wave Quantum Memories with a Dynamical Symmetry. *Physical Review Letters* **91**, 147903 (2003).
35. Yang, C.-P., Chu, S.-I. & Han, S. Possible realization of entanglement, logical gates, and quantum-information transfer with superconducting-quantum-interference-device qubits in cavity QED. *Physical Review A* **67**, 042311 (2003).
36. Yang, C.-P., Chu, S.-I. & Han, S. Quantum Information Transfer and Entanglement with SQUID Qubits in Cavity QED: A Dark-State Scheme with Tolerance for Nonuniform Device Parameter. *Physical Review Letters* **92**, 117902 (2004).
37. Zhou, Z., Chu, S.-I. & Han, S. Suppression of energy-relaxation-induced decoherence in Λ-type three-level SQUID flux qubits: A dark-state approach. *Physical Review B* **70**, 094513 (2004).
38. You, J. Q. & Nori, F. Atomic physics and quantum optics using superconducting circuits. *Nature* **474**, 589 (2011).
39. Falci, G. *et al*. Design of a Lambda system for population transfer in superconducting nanocircuits. *Physical Review B* **87**, 214515 (2013).
40. Inomata, K. *et al*. Microwave Down-Conversion with an Impedance-Matched ΛSystem in Driven Circuit QED. *Physical Review Letters* **113**, 063604 (2014).
41. Margalit, L., Rosenbluh, M. & Wilson-Gordon, A. D. Degenerate two-level system in the presence of a transverse magnetic field. *Physical Review A* **87**, 033808 (2013).
42. Zhang, H.-B., Yang, G., Huang, G.-M. & Li, G.-X. Absorption and quantum coherence of a degenerate two-level system in the presence of a transverse magnetic field in different directions. *Physical Review A* **99**, 033803 (2019).
43. Liu, Y.-x, You, J. Q., Wei, L. F., Sun, C. P. & Nori, F. Optical Selection Rules and Phase-Dependent Adiabatic State Control in a Superconducting Quantum Circuit. *Physical Review Letters* **95**, 087001 (2005).
44. Zhou, B. B. *et al*. Accelerated quantum control using superadiabatic dynamics in a solid-state lambda system. *Nature Physics* **13**, 330–334 (2016).
45. Messiah, A. *Quantum Mechanics*. (Wiley, New York, 1976).
46. Wajnflasz, J. & Pick, R. Transitions "Low Spin"-"High Spin" Dans Les Complexes De Fe2+. *J. Phys. Colloques* **32**, C1 (1971).
47. Press, W. H. *et al*. *Numerical Recipes in C++: The Art of Scientific Computing* (Cambridge University Press, 2002).
48. Nishimori, H. & Ortiz, G. *Elements of Phase Transitions and Critical Phenomena*. Oxford Graduate Texts (OUP Oxford, 2011).
49. Bapst, V., Foini, L., Krzakala, F., Semerjian, G. & Zamponi, F. The quantum adiabatic algorithm applied to random optimization problems: The quantum spin glass perspective. *Physics Reports* **523**, 127–205 (2013).
50. Gardner, E. 1-s2.0-0550321385903748-main. *Nuclear Physics B* **257**, 747 (1985).
51. Läuchli, A., Mila, F. & Penc, K. Quadrupolar Phases of the S = 1 Bilinear-Biquadratic Heisenberg Model on the Triangular Lattice. *Physical Review Letters* **97**, 087205 (2006).
52. Smerald, A. & Shannon, N. Theory of spin excitations in a quantum spin-nematic state. *Physical Review B* **88**, 184430 (2013).
53. Lechner, W., Hauke, P. & Zoller, P. A quantum annealing architecture with all-to-all connectivity from local interactions. *Science Advances* **1**, e1500838 (2015).
54. Glaetzle, A. W., van Bijnen, R. M. W., Zoller, P. & Lechner, W. A coherent quantum annealer with Rydberg atoms. *Nat Commun* **8**, 15813 (2017).

Acknowledgements
We thank R. van Bijnen, W. Lechner, Y. Matsuzaki, T. Ishikawa, T. Yamamoto, and T. Nikuni for fruitful discussions and comments. Two of the authors (S.W. and S.K.) were supported by Nanotech CUPAL, Japan Science and Technology Agency (JST). Y.S. and S.K. were supported by the New Energy and Industrial Technology Development Organization (NEDO), Japan.

Author contributions
S.W., Y.S. and S.K. designed the study, S.W. and Y.S. contributed to theoretical calculations, S.W. performed numerical simulation and S.W., Y.S. and S.K. contributed to writing the manuscript.

Competing interests
The authors declare no competing interests.

Additional information
Supplementary information is available for this paper at https://doi.org/10.1038/s41598-019-56758-4.

Correspondence and requests for materials should be addressed to S.W.

Reprints and permissions information is available at www.nature.com/reprints.

Publisher's note Springer Nature remains neutral with regard to jurisdictional claims in published maps and institutional affiliations.